Measurement of Threshold Voltages in PTP Structures and Estimation of P-stop Densities Across an ATLAS18 Silicon Strip Sensor Wafer Using TCAD Simulations

Y. Unno^{b,*}, P.S. Miyagawa^e, A. Awais^e, E. Bach^e, G.A. Beck^e, A.J. Bevan^e, Z. Chen^e, I. Dawson^e, V. Fadeyev^d, P. Federicova^e, J. Kozakova^e, J. Kroll^e, R.R. Marcelo Gregorio^{e,1}, M. Mikestikova^e, M. Ullan^e, S.C. Zenz^e

J. Kozakova^e, J. Kroll^e, R.R. Marcelo Gregorio^{e,1}, M. Mikestikova^e, M. Ullan^e, S.C. Zenz^e

Institute of Particle and Nuclear Study, High Energy Accelerator Research Organization (KEK), 1-1 On, Tsukuba, Ibaraki 305-0801, Japan Institute of Physics, Academy of Sciences of the Czech Republic, Na Slovance 2, 18221 Prague 8, Czech Republic Granta Cruz, Chaptic Particle Physics (SCIPP), University of California, Santa Cruz, Chaptic Physics Research Centre, Queen Mary University of London, G.O. Jones Building, Mile End Road, London E1 4NS, United Kingdom



Abstract - A total of 24,010 AC-coupled silicon strip sensors, consisting of n-type strips in p-type silicon and referred to as ATLAS18, are currently in production for installation in the upgraded ATLAS Inner Tracker (ITk).

In n-in-p strip sensors, a dense p-type region (e.g., p-stop implant) is essential for electrically isolating the n-type strips from a conductive inversion layer between the strips, caused by positive interface charges.

The punch-through protection (PTP) structure is implemented at one end of each strip to protect the AC-coupling capacitor in the event of large currents flowing into the strips. During quality assurance (QA) testing, we occasionally observed a deviation in the threshold voltage (VPT) of the PTP structure in the test chips located at a corner of the wafer perimeter, with a shift of four standard deviations or more below the mean.

To evaluate the variation of V_{PT} across a wafer, we selected two main sensors, each processed in a different furnace, where V_{PT} measurements in the QA test chips were still near the mean value. One sensor exhibited a flat distribution of V_{PT} measurements, while the other showed a non-uniform, parabolic distribution, with a shift of four standard deviations toward the wafer edge.

TCAD simulations were used to analyse $V_P r$ as a function of p-stop density, confirming that the V_{PT} correlates well with the p-stop density. By setting the nominal p-stop density ($4 \times 10^{12} \, \mathrm{cm}^{-2}$) to correspond to the mean V_{PT} value, the p-stop density at the wafer edge, which is four standard deviations away from the mean, is estimated to be approximately half ($2 \times 10^{12} \, \mathrm{cm}^{-2}$). A p-stop density of $2 \times 10^{12} \, \mathrm{cm}^{-2}$ should still be sufficient to ensure isolation, even after irradiation, and in the presence of interface charges as high as $1 \times 10^{12} \, \mathrm{cm}^{-2}$.

Introduction – A total of 24,010 AC-coupled silicon strip sensors are currently in production, consisting of n-type strips in p-type silicon, referred to as ATLAS18, for installation (17,888 sensors) in the outer layer of the upgraded ATLAS Inner Tracker (ITk) [1].

In n-in-p strip sensors, a dense p-type region (e.g., p-stop implant) is essential for electrically isolating the n-type strips from a conductive inversion layer in the surface of silicon between the strips which is caused by positive interface charges.

writion is caused by positive interface charges.

A punch-through protection (PTP) structure, a narrow gap between the strip and the bias rail implants, is implemented at one end of each strip to protect the AC-coupling capacitor in the event of large currents flowing into the strip. The PTP structure creates a current flow channel between the strip and the bias rail implants despite the presence of the p-stop implant, in parallel with the bias resistor. A trace of bias resistor is designed to overlap the PTP region, functioning as a gate and ensuring a low PTP threshold voltage and fast turn-on [2].

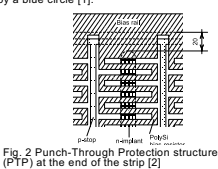
During quality assurance (QA) testing, we occasionally observed² in the QA test chips that the threshold voltage (V_P) of PTP structure deviated by approximately 4 times the standard deviations (sigma) below the mean, where V_{PT}(QA) for those within acceptance limits is ~15 V (mean) and ~0.8 V (sigma). The QA test chips are located at the corner of the perimeter of the 6-inch wafer.

To evaluate the Ver variation across a wafer, we measured the strips in the main sensors. The main sensor is designed with approximately 1,280 strips, each having a typical strip pitch of 75 μ m and containing either 2 or 4 segments per strip.

We used TCAD simulations to analyze the dependence of V_{PT} on pstop density and other factors.

segment 2

Water Layout of the barrel sensor, short-stri type (SS). Strips are arranged vertically, and consist of 4 segments. OA testchips are diced along the orange line, one set per wafer, indicate by a blue circle [1].



Variation of V_{PT} across a wafer – We selected two main sensors, each processed with a different furnace, and measured the V_{PT} of the strips to probe the variation across the wafer. In this setup, segments 1 (Seg 1) and 4 represent the PTP structure at the ends of the sensor, while segment 2 represents the middle. VPA53553-W03492, processed with furnace B, showed flat V_{PT} distributions. VPA50932-W03132, processed with furnace A, showed non-uniform, parabolic V_{PT} distributions across the wafer, with V_{PT} approximately 4 standard deviations below the mean toward the edge in segment 2.

The measured V_{PT} of the QA test chips of these wafers (in the red circle) were still near the mean value, ~15 V.

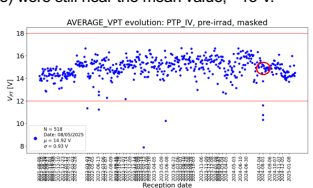


Fig. 3 Trend plot of $V\!P\!T$ over the course of production [5]. The acceptance limits are between 12 V and 18 V for the lower and upper bounds, respectively.

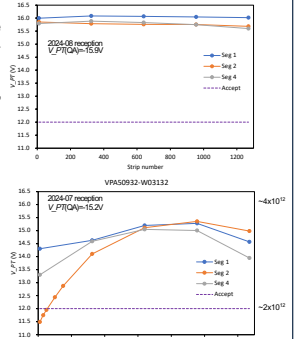


Fig. 4 VPT measurements obtained by sampling strips across the wafer, with furnace B (top) and A (bottom).

TCAD model of the PTP structure – We used the TCAD 3D device simulator, HyDeLEOS VER. 8.5k [3]. The PTP structure is implemented in 2D geometry (Fig. 5) with the major parameters used in the simulations listed in Table 1.

Table 1. Major parameters of PTP structure in TCAD simulations

Silicon bulk: p-type, 3 k Ω cm, 320 μ m n-strip (Nsub1: n+ implant) Bias rail (Nsub2: n+ implant) Bias voltages: 0 V to the bias rail, -400 V applied to the backplane

- sias resistor: Al (partially high resistivity, equivalent to PolySi) $1.5 \, \text{M}\Omega \text{ resistance } (R_b)$ The trace of the bias resistor functions as a gate to the PTP structure

structure
Oxide thickness (tSio2): 0.15 µm
Oxide-silicon interface charge: 8x10¹0 cm²
p-stop (wPsub: p· implant): ~6 µm
- nominal surface density: 4x10¹2 cm²
PTP gap (ggap): ~7 µm each

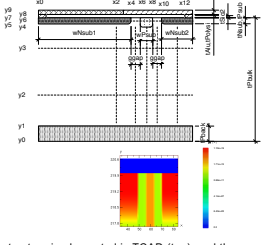


Fig. 5 PTP structure implemented in TCAD (top), and the graphical display of doping densities (bottom), both not to

PTP structure resistance – The current flow between the bias rail (Nsub2) and the strip implant (Nsub1) was simulated by varying the strip implant potential (*Vsuip*), while keeping the bias rail potential at 0 V and the backplane at 400 V.

The PTP resistance was defined as RPT = Istrip / Vstrip

Rer is shown as a function of V_{ship} (Fig. 6). The threshold voltage for PTP turn-on (Ver) is defined as the strip potential at which Rer is half of the bias resistance (1/2 R_b =

In the simulation, V_{strip} had a negative potential. When expressing V_{PT} , we take the absolute value.

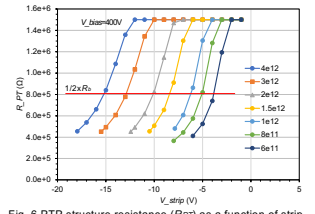
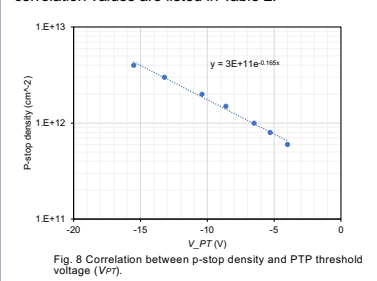


Fig. 6 PTP structure resistance (RPT) as a function of strip potential $V_{\it strip}$, with variations in p-stop density.

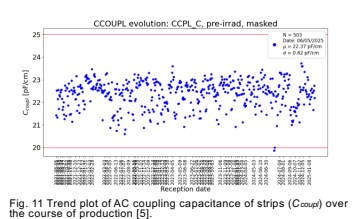
The turn-on condition is visualized in the electron density. For a p-stop density of 4×10^{12} , at $V_{strip}=-1$ V, it is not visible, while at -16 V, a thin inversion layer becomes visible at the surface, connecting the strip and bias rail implants across the p-stop area (Fig. 7) Correlation between p-stop density and V_{PT} – From the plot (Fig. 6), V_{PT} is obtained for p-stop densities ranging from 4×10^{12} to 6×10^{11} cm²² (Fig. 8). The p-stop density correlates exponentially with V_{PT} .

If the p-stop density 4 × 10¹² cm² is scaled to *V_{PT}* ~ 16 V, *V_{PT}* ~ 12 V corresponds to a p-stop density of approximately 2 × 10¹² cm². The corresponding p-stop density is shown on the second axis in Fig. 4. Typical correlation values are listed in Table 2.



Oxide thickness – Oxide thickness beneath the bias resistor is another factor that affects V_{PT} , as the potential difference between the resistor and the p-stop functions as a gate. The dependence of R_{PT} on the oxide thickness was simulated (Fig. 9). VPT shows a linear correlation with the oxide thickness (Fig. 10).

In the process, the variation in oxide thickness is estimated to be small, approximately $0.15\pm0.004~\mu m$, based on the variation in AC coupling capacitance (Fig. 11). The oxide thickness is not expected to be a major contributor to the variation in V_{PT} . Additionally, the p-stop density is independent of the oxide thickness.



Radiation damage effect – Irradiation with γ rays, charged particles, and neutral particles induces radiation damage in the PTP structure, such as an increase in the interface charge at the oxide-silicon interface and the space charge in the silicon bulk.

The dependence of Rer on the interface charge was simulated for a p-stop density of 2×10^{12} cm⁻² (Fig. 12). Ver shows linear correlation with the interface charge. Isolation in the PTP structure is lost when the interface charge exceeds 1×10^{12} cm⁻².

charge exceeds 1 × 10 × 611 .

An increase in the space charge from 4 × 10¹² cm³ (non-irradiated) to 2.2 × 10¹³ cm³ (after a fluence of 1 × 10⁵ neq/cm²) leads to an increase in VPr by 3 V under a bias voltage of 400 V (Fig. 13). This increase is due to a stronger electric field caused by the larger space charge. The difference is equivalent to a reduction in the interface charge of ~5 × 10¹¹ cm².

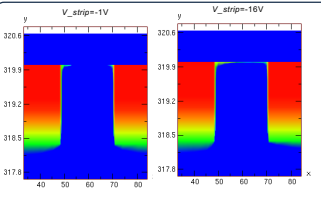
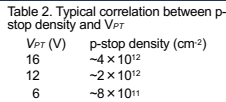


Fig. 7 Plot of the electron density in the PTP region at V_{strip} = -1V (left) and -16V (right), where the latter corresponds to R_{PT} being approximately ½ R_{b} .



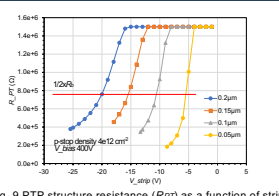
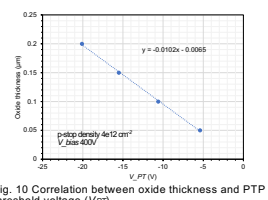


Fig. 9 PTP structure resistance (RPT) as a function of strip potential V_{strip}, with variations in oxide thickness.



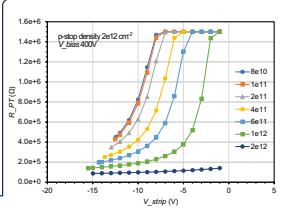
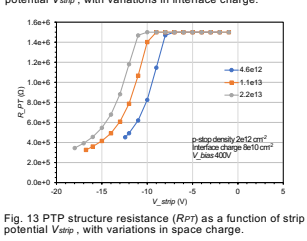


Fig. 12 PTP structure resistance (RPT) as a function of strip potential V_{strip} , with variations in interface charge.



Conclusion – We observed rare but occasional deviations in the threshold voltage (*VPI*) of the punch-through protection (PTP) structure in test chips during quality assurance (QA) process of the ATLAS18 strip sensor production.

Of the two main sensors selected, each processed in a different furnace, one sensor exhibited a flat distribution across the wafer, while the other showed a non-uniform, parabolic distribution with a four-standard-deviation shift toward the wafer edge.

TCAD simulations confirm that V_{PT} correlates well with the p-stop density. By setting the nominal p-stop density (-4×10^{12} cm $^{-2}$) to correspond to the mean V_{PT} value (-16 V), the p-stop density at the water edge, four standard deviations away from the mean, is estimated to be approximately half (-2×10^{12} cm $^{-2}$).

The low value of 2×10¹² cm⁻² should still be sufficient to ensure strip isolation, even after radiation damage, and in the presence of oxide—silicon interface charges with densities as high as 1×10¹² cm⁻².

Acknowledgements
We gratefully acknowledge Y. Abo, M. Metzger, and the HPK team for their close communication during the production of ATLAS18 strip sensors. This work was supported by the European Structural and Investment Funds and the Ministry of Education, Youth and Sports of the Czech Republic via projects LM2023040 CERN-CZ, and FORTE – Czl.02.10.10022_0880004632 in Czechia, the Spanish R&D grant PID2021-126327OBC22, funded by MICIU AEI10.13039501100011033 and by ERDFEU in Spain, STFC grants STW0004741, STS00095X1, STX0014311, ST/R00241X11 in UK, and the US Department of Energy, grant DE-SC0010107, in USA.

References
[1] Y. Unno et al., "Specifications and pre-production of n+in-p large-format strip sensors fabricated in 6-inch silicon wafers, ATLAS1B, for the Inner Tracker of the ATLAS Detector for High-Luminosity Large Hadron Collider," JINST 18, no.03, 103,008 (2023), https://doi.org/10.1088/1748-022/118/03/103088 misspace for long-strip barrel section of ATLAS TR strip detector, "Nucl. Instrum. Meth. A 989, 164928 (2021), https://doi.org/10.1016/j.nima.2020.164928; Y. Unno, et al. "TALAS1T/L-S4 large-format prototype sensors for very high radiation environments — ATLAS1Z design and initial results," Nucl. Instrum. Meth. A 765, 80-90 (2014), https://doi.org/10.1016/j.nima.2014.06.086; M. Mikestikova, et al. "Study of surface properties of ATLAS1Z strips sensors and their radiation resistance," Nucl. Instrum. Meth. A 831, 197-206 (2016), https://doi.org/10.1016/j.nima.2016.03.056
[3] Keiu Dinversity, TCAD R&D Center (TRIECC), "HybeLEGS Ver, 8.5k User's manual", 2019
[4] Y. Unno, et al. "Analysis of MoS capacitor with player with TCAD simulation", Nucl. Instrum. Meth. A 1064, 170045
[5] (2024), https://doi.org/10.1016/j.nima.2024.170045
[5] (2025), https://doi.org/10.1016/j.nima.2024.170045
[6] (2016), https://doi.org/10.1016/j.nima.2024.15045; R. Orr, et al. Quality Assurance during production of the ATLAS18 TIK strip sensors", Nucl. Instrum. Meth. A 1064, 169435 (2024), https://doi.org/10.1016/j.nima.2024.169435; R. Orr, et al. Quality Assurance during production of the ATLAS18 TIK strip sensors", presented in this conference

*Corresponding author (e-mail: yoshinobu.unno@kek.jp)
*Current address: Department of Nuclear Physics & Accelerator Applications, The Australian National University, Canberra ACT 2600, Australia
*A decrease in p-stop density was observed in the MOS capacitor test structure with the p-layer during production [4].